Naive T cells are dispensable for memory CD4+ T cell homeostasis in progressive simian immunodeficiency virus infection

Afam A. Okoye,[1] Mukta Rohankhedkar,[1] Chike Abana,[1] Audrie Pattenn,[1] Matthew Reyes,[1] Christopher Pexton,[1] Richard Lum,[1] Andrew Sylwester,[1] Shannon L. Planer,[1] Alfred Legasse,[1] Byung S. Park,[2] Michael Piatak Jr.,[3] Jeffrey D. Lifson,[3] Michael K. Axthelm,[1] and Louis J. Picker[1]

[1]Vaccine and Gene Therapy Institute, Departments of Pathology and Molecular Microbiology and Immunology, Oregon National Primate Research Center, Oregon Health & Science University, Beaverton, OR 97006
[2]Division of Biostatistics, Department of Public Health and Preventive Medicine, Oregon Health & Science University, Portland, OR 97239
[3]AIDS Vaccine Program, SAIC Frederick, Inc., National Cancer Institute-Frederick, Frederick, MD 21702

The development of AIDS in chronic HIV/simian immunodeficiency virus (SIV) infection has been closely linked to progressive failure of CD4+ memory T cell (T_M) homeostasis. CD4+ naive T cells (T_N) also decline in these infections, but their contribution to disease progression is less clear. We assessed the role of CD4+ T_N in SIV pathogenesis using rhesus macaques (RMs) selectively and permanently depleted of CD4+ T_N before SIV infection. CD4+ T_N–depleted and CD4+ T_N–repleted RMs were created by subjecting juvenile RMs to thymectomy versus sham surgery, respectively, followed by total CD4+ T cell depletion and recovery from this depletion. Although thymectomized and sham-treated RMs manifested comparable CD4+ T_M recovery, only sham-treated RMs reconstituted CD4+ T_N. CD4+ T_N–depleted RMs responded to SIVmac239 infection with markedly attenuated SIV-specific CD4+ T cell responses, delayed SIVenv-specific Ab responses, and reduced SIV-specific CD8+ T cell responses. However, CD4+ T_N–depleted and –repleted groups showed similar levels of SIV replication. Moreover, CD4+ T_N deficiency had no significant effect on CD4+ T_M homeostasis (either on or off anti-retroviral therapy) or disease progression. These data demonstrate that the CD4+ T_N compartment is dispensable for CD4+ T_M homeostasis in progressive SIV infection, and they confirm that CD4+ T_M comprise a homeostatically independent compartment that is intrinsically capable of self-renewal.

CORRESPONDENCE
Louis J. Picker:
pickerl@ohsu.edu

Abbreviations used: ART, antiretroviral therapy; BAL, bronchoalveolar lavage lymphocyte; OI, opportunistic infection; pi, post infection; pvl, plasma viral load; RM, rhesus macaque; SIV, simian immunodeficiency virus.

Progressive CD4+ T cell depletion is a hallmark of HIV and pathogenic simian immunodeficiency virus (SIV) infection, and it is thought to play a primary role in mediating the immunodeficiency that characterizes AIDS (Douek et al., 2003). Although these viruses target and destroy CD4+ T cells, the pathophysiology of the slow progressive depletion mediated by typical CCR5-tropic HIV/SIV involves a complex interplay between CD4+ T cell destruction (both direct killing by viral infection and indirect killing of uninfected cells by activation-related apoptosis) and regeneration, the latter initiated by both homeostatic mechanisms and immune activation (Grossman et al., 2006; Catalfamo et al., 2011). Massive viral replication in primary infection preferentially targets CCR5-expressing CD4+ transitional effector memory T cells (T_{TrEM}) and fully differentiated effector memory T cells (T_{EM}), causing profound depletion of these CD4+ T cell populations in extra-lymphoid effector sites (Brenchley et al., 2004; Mattapallil et al., 2005). However, CCR5-nonexpressing secondary lymphoid tissue–based central memory CD4+ T cells (T_{CM}) are relatively spared from this initial destruction and provide precursors for both their own homeostasis and partial CD4+ T_{TrEM} and T_{EM} regeneration (Picker et al., 2004; Okoye et al., 2007; Grossman and Picker, 2008;

The Rockefeller University Press $30.00
J. Exp. Med. Vol. 209 No. 4 641-651
www.jem.org/cgi/doi/10.1084/jem.20112071

The Journal of Experimental Medicine

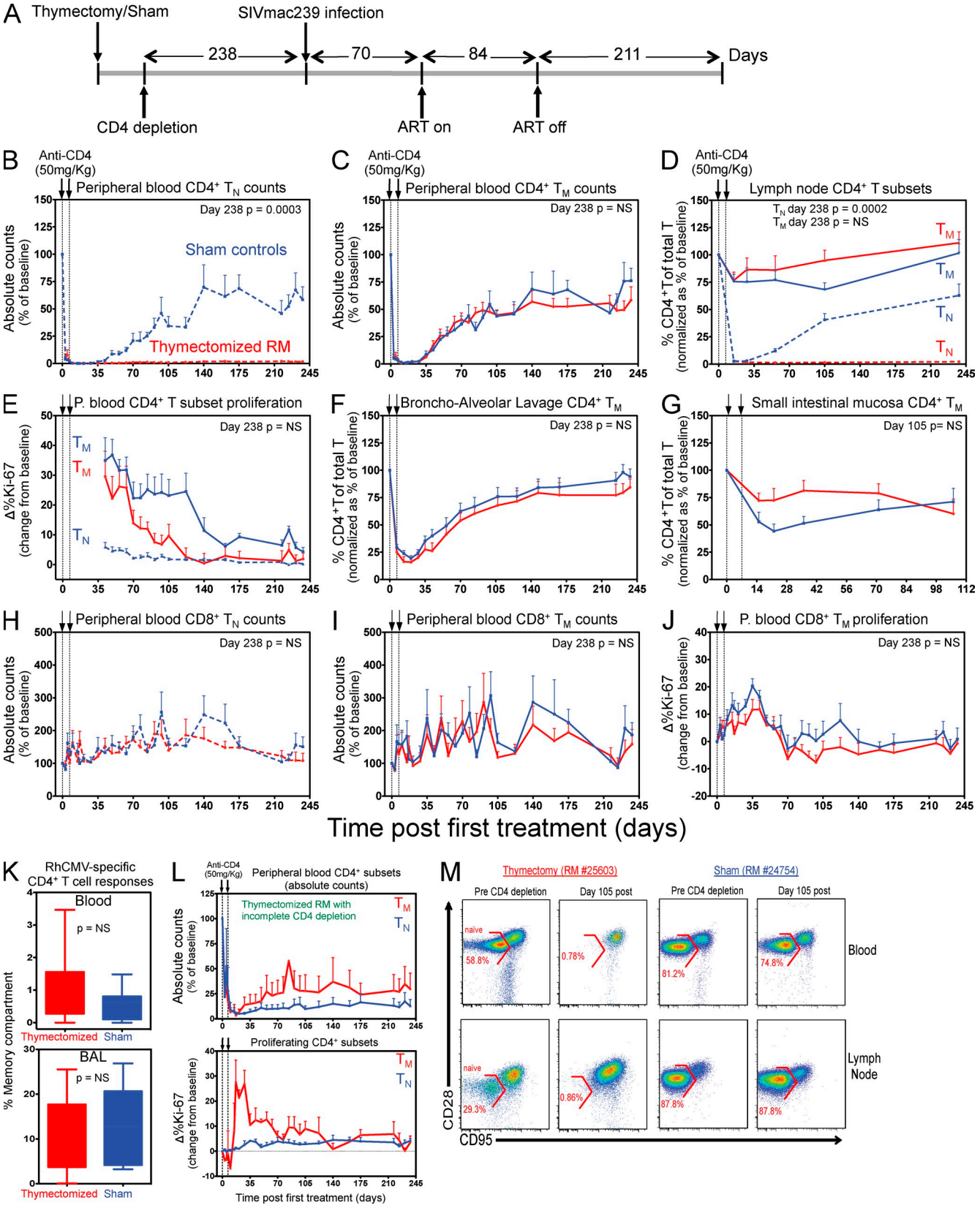

Figure 1. Thymectomy abrogates CD4⁺ T_N recovery after antibody-mediated CD4⁺ T cell depletion. (A) Schematic representation of the experimental protocol used in this study. (B–J) Analysis of CD4⁺ and CD8⁺ T_N (dashed lines) and T_M (solid lines) population dynamics after mAb huOKT4A treatment

Mason et al., 2008). In the absence of such CD4+ T_{TrEM} and T_{EM} regeneration, SIV-infected rhesus macaques (RMs) manifest rapid progression to AIDS, whereas in its presence, RMs survive into chronic infection, maintaining sufficient CD4+ T cell effector function to hold opportunistic infections (OIs) at bay (Picker et al., 2004; Okoye et al., 2007; Grossman and Picker, 2008). This tenuous immune competence is unstable, as over time, lymphoid microenvironments are destroyed (Zeng et al., 2011) and CD4+ T_{CM} populations progressively decline, reducing CD4+ T_{TrEM} and T_{EM} production until these effector populations fall below a crucial threshold associated with the onset of AIDS (Okoye et al., 2007). Thus, although CD4+ T_{TrEM} and T_{EM} comprise the proximate effectors that directly mediate most of the immunological functions of CD4+ T cell lineage, the progressive homeostatic failure of the T_{CM} population and the consequent inability of this population to produce sufficient numbers of T_{TrEM} and T_{EM} appear to play a major role in determining the tempo disease progression to AIDS.

In RMs infected with pathogenic, CCR5-tropic SIV, CD4+ T_{TrEM} and T_{EM} populations can collapse and overt AIDS can ensue in the presence of essentially normal CD4+ naive T cell (T_N) populations (Picker et al., 2004; Okoye et al., 2007), suggesting that T_N are not able to directly support T_{TrEM} and T_{EM} regeneration. However, it has been suggested that CD4+ T_{CM} population stability is dependent on continuous recruitment of new cells from the T_N pool (Nishimura et al., 2007). In this regard, the CD4+ T_{TrEM} and T_{EM} most relevant to HIV/SIV infection and AIDS are those specific for HIV/SIV itself and for the pathogens responsible for OIs, which are either persistent or environmentally ubiquitous agents that are continuously or periodically available to drive de novo T_M production from T_N precursors (Vezys et al., 2006). Alternatively, T_{CM} include cells with stem-like qualities (Gattinoni et al., 2011), and it is possible that CD4+ T_{CM} homeostasis is more dependent on proliferation and survival of T_{CM} populations established before infection.

To determine the role of CD4+ T_N recruitment in CD4+ T_{CM} population stability in progressive SIV infection, we developed a new RM model in which the CD4+ T_N compartment of healthy juvenile RMs is specifically, permanently, and profoundly depleted. Such CD4+ T_N-depleted RMs were created by thymectomizing juvenile animals, followed by treatment with the depleting anti-CD4 huOKT4 mAb (Engram et al., 2010), and then allowing ~7 mo for maximal CD4+ T_M regeneration. Control animals (CD4+ T_N-repleted RMs) were sham-thymectomized, but otherwise treated identically. CD4+ T_M regeneration was comparable in both groups, but only the sham-thymectomized group manifested CD4+ T_N recovery. Strikingly, upon infection with the SIVmac239, we observed no significant differences between these groups in the kinetics and magnitude of SIV replication, CD4+ T_M decline, or time to AIDS, despite a marked attenuation of the SIV-specific CD4+ T cell response and significant impairments in the development of both the SIV-specific CD8+ T cell and Ab responses in the CD4+ T_N-depleted RMs. These data demonstrate that the CD4+ T_N compartment is not required for CD4+ T_M homeostasis/regeneration in pathogenic SIV infection, and they confirm the essential role of CD4+ T_{CM} homeostasis in AIDS pathogenesis.

RESULTS AND DISCUSSION

Establishment of permanent selective CD4+ T_N cell deficiency by anti-CD4 mAb–mediated CD4+ T cell depletion of thymectomized juvenile RMs

Previous work has demonstrated that abrogation of thymopoiesis—and, consequently, de novo T_N production—by preinfection thymectomy does not have a significant impact on the pathogenesis of SIV infection (Arron et al., 2005). However, thymectomy would not affect previously established T_N, and the RMs in these studies would have had a large pool of CD4+ T_N at the time of SIV infection that would have been capable of supporting CD4+ T_M homeostasis post infection (pi). To more rigorously assess the ability of CD4+ T_N to contribute to CD4+ T_M homeostasis in the setting of pathogenic SIV infection, we sought to create an RM model in which the CD4+ T_N compartment is selectively ablated. We based our approach on the hypothesis that the thymus is the only significant source of de novo T_N production in primates, and on previous observations that CD4+ T_N populations in euthymic juvenile RMs reconstitute after efficient depletion by treatment with mAb huOKT4 (Arron et al., 2005; Engram et al., 2010). Our strategy was to perform thymectomy or sham surgery on groups of 3–5-yr-old RMs, followed by mAb huOKT4-mediated CD4+ lymphocyte depletion and postdepletion recovery to a stable endpoint (Fig. 1 A). We expected CD4+ T_N, but not CD4+ T_M, reconstitution to depend on the presence of a functioning thymus.

in RMs with complete initial CD4+ T cell depletion in blood that were previously subjected to thymectomy (red, $n = 9$) versus sham surgery (blue, $n = 9$). Results (mean + SEM) are shown as percentage of baseline, or for percentage of Ki-67+, change (Δ) from baseline (see Materials and methods). Note that T cells in BAL and small intestinal mucosa are essentially all T_M (Pitcher et al., 2002). The significance of differences in these parameters between the thymectomized and sham-treated groups at day 238 (day 105 for small intestinal mucosa cells) after first mAb dose was assessed as described in the Materials and methods (significant p-values shown; NS, nonsignificant). (K) Comparison of the frequency of RhCMV-responsive cells within the CD4+ memory populations of blood and BAL at day 238 after depletion. Shown are box plots, with boxes and whiskers indicating interquartile ranges (25^{th}–75^{th} percentiles) and 10^{th}–90^{th} percentile values, respectively. (L) Analysis of CD4+ T_N (blue) and CD4+ T_M (red) dynamics (absolute counts and proliferative fraction; mean + SEM) in three thymectomized RMs with incomplete initial CD4+ T cell depletion in blood (mean of 95% at day 21) after mAb huOKT4A treatment. (M) Flow cytometric profiles of blood and peripheral LN T_N versus T_M subsets from representative thymectomized and sham-treated RMs before and after complete CD4+ T cell depletion. The CD28 versus CD95 profiles shown were gated on CD3+/CD4+ small lymphocytes with red lines delineating the position of the T_N cluster. Multiparameter analysis (see Materials and methods) was used for the actual quantification of T_N versus T_M, with the percentage of T_N shown in red.

As shown in Fig. 1 (B–D), 18 RMs (9 thymectomized and 9 sham-treated) receiving mAb huOKT4 treatment (out of a total of 26, with 13 in each group) achieved complete depletion of $CD4^+$ T_N and T_M in blood and $CD4^+$ T_N in LN through day 35 after treatment. As expected, $CD4^+$ T_N numbers subsequently rebounded in blood and LN of sham-treated controls, but not in the thymectomized RMs. Regenerating $CD4^+$ T_N in the blood of the sham-treated RMs showed a relatively small increase in their proliferative fraction (Ki-67^+; Pitcher et al., 2002) from before depletion (Fig. 1 E, dashed line), consistent with the thymus (rather than peripheral regeneration) being the primary source of $CD4^+$ T_N recovery in these RMs. After mAb huOKT4 treatment, $CD4^+$ T_M were incompletely depleted in LN (Fig. 1 D) and effector sites (lung airspace and small intestinal lamina propria; Fig. 1, F and G) of both thymectomized and sham-treated RMs, providing a substrate for subsequent T_M regeneration. Indeed, in both RM groups, $CD4^+$ T_M reappeared in the blood at ~35 d after depletion and recovered to a similar degree (>50% of pre-depletion levels) over the subsequent 120 d (Fig. 1 C). Both groups also manifested stabilization of $CD4^+$ T_M recovery at ~75% of pre-depletion levels in the effector sites (Fig. 1, F and G). $CD4^+$ T_M recovery was clearly associated with peripheral homeostatic expansion, as the fraction of circulating $CD4^+$ T_M expressing Ki-67 was dramatically increased from pretreatment baseline levels during early recovery, falling back to near baseline levels upon stabilization of $CD4^+$ T_M numbers at 140–160 d after depletion (Fig. 1 E, solid lines). Both thymectomized and sham-treated RMs manifested similar frequencies of RhCMV-specific $CD4^+$ T cells in blood and lung airspace after recovery (Fig. 1 K), in keeping with the essentially equivalent $CD4^+$ T_M regeneration in these RMs.

To ascertain whether homeostatic activation and expansion of $CD4^+$ T_N with memory conversion contributed to $CD4^+$ T_M recovery (Sener et al., 2009), we analyzed $CD4^+$ T_N and T_M dynamics in three thymectomized RMs in which $CD4^+$ T cell depletion in blood fell just short of completion, allowing analysis throughout the regeneration period (Fig. 1 L). After treatment of these RMs, residual $CD4^+$ T_M showed regeneration similar to that previously described for the RMs with complete depletion, associated with a marked increase in proliferative fraction, whereas residual $CD4^+$ T_N showed (at all time points) very limited regeneration associated with much smaller changes in proliferative fraction. As proliferating T_N serve as the substrate for T_N-derived pseudo-memory differentiation, and as this process might be expected to deplete the phenotypically defined T_N cells in the absence of thymic renewal, these data argue against a significant contribution of this process to $CD4^+$ T_M recovery under the conditions of this experiment.

HuOKT4 mAb treatment had little effect on $CD8^+$ T_N numbers in blood in either RM group (Fig. 1 H), whereas $CD8^+$ T_M from both groups displayed a variable, modest increase in numbers in blood that was associated with a transient increase in proliferative fraction, consistent with a response to common homeostatic cytokines (Fig. 1, I and J). Overall, these data demonstrate the ability to generate RMs with profound systemic $CD4^+$ T_N cell deficiency ($CD4^+$ T_N-depleted), as well as a matched control group that has undergone similar treatment but has regenerated a $CD4^+$ T_N compartment that is at, or very near, pretreatment baseline levels ($CD4^+$ T_N-repleted; Fig. 1 M).

SIV replication dynamics and the development of SIV-specific adaptive immunity in $CD4^+$ T_N-depleted versus -repleted RMs

Reconstitution of all $CD4^+$ T cell subsets reached a plateau in both $CD4^+$ T_N-depleted and -repleted RM cohorts at ~140 d after depletion (Fig. 1) and, after documenting an additional 95 d of population stability, both cohorts ($n = 9$ each) were challenged with highly pathogenic SIVmac239 by i.v. injection. Our strategy was to allow the infection to proceed without interference for 70 d to allow comparison of the ability of each cohort to: establish plasma viral load (pvl) set-point; develop adaptive SIV-specific immunity; and stabilize early plateau-phase $CD4^+$ T_M population dynamics. At day 70 pi, we administered the anti-retroviral drugs tenofovir (30 mg/kg/d) and emtricitabine (50 mg/kg/d) to assess the regenerative potential of $CD4^+$ T_M associated with (partial) control of viral replication. These drugs were discontinued at day 154 pi, and the cohorts were subsequently compared for viral replication and lymphocyte population dynamics until the onset of clinical AIDS or for 211 d of untreated chronic infection (1 yr of infection overall; Fig. 1 A).

We also analyzed a contemporaneous group of six unmanipulated RMs given the same SIVmac239 challenge and followed for key parameters of infection through day 70 pi, so as to determine whether the sham surgery and/or the subsequent huOKT4 treatment and recovery from that treatment of the $CD4^+$ T_N-repleted control group affected the ability of these RMs to handle or respond to SIVmac239 infection. As shown in Fig. 2 A, this comparison demonstrated no significant differences between the unmanipulated RMs and the $CD4^+$ T_N-repleted RM cohort with respect to: peak and early plateau pvl; $CD4^+$ T_M depletion in blood and bronchoalveolar lavage lymphocytes (BALs) at day 70 pi; the increase in $CD4^+$ T_M proliferative fraction (Ki-67^+) from baseline to day 70; and development of SIV-specific $CD8^+$ T cell responses.

At the end of the recovery period after huOKT4 treatment, the $CD4^+$ T_N-depleted cohort manifested almost a complete absence of circulating $CD4^+$ T_N cells. Importantly, no $CD4^+$ T_N regeneration was observed throughout the entire course of SIV infection in the $CD4^+$ T_N-depleted cohort, in sharp contrast to the $CD4^+$ T_N-repleted RMs (Fig. 2 B). $CD4^+$ T_N lack CCR5 expression, and are thus not primary targets of CCR5-tropic SIV (Picker et al., 2004). Therefore, given the essentially equivalent $CD4^+$ T_M populations in the $CD4^+$ T_N-depleted and -repleted cohorts (Fig. 1), it is not surprising that the absence of $CD4^+$ T_N in the former group had no effect on peak pvl (Fig. 2 C). More surprising was the observation that

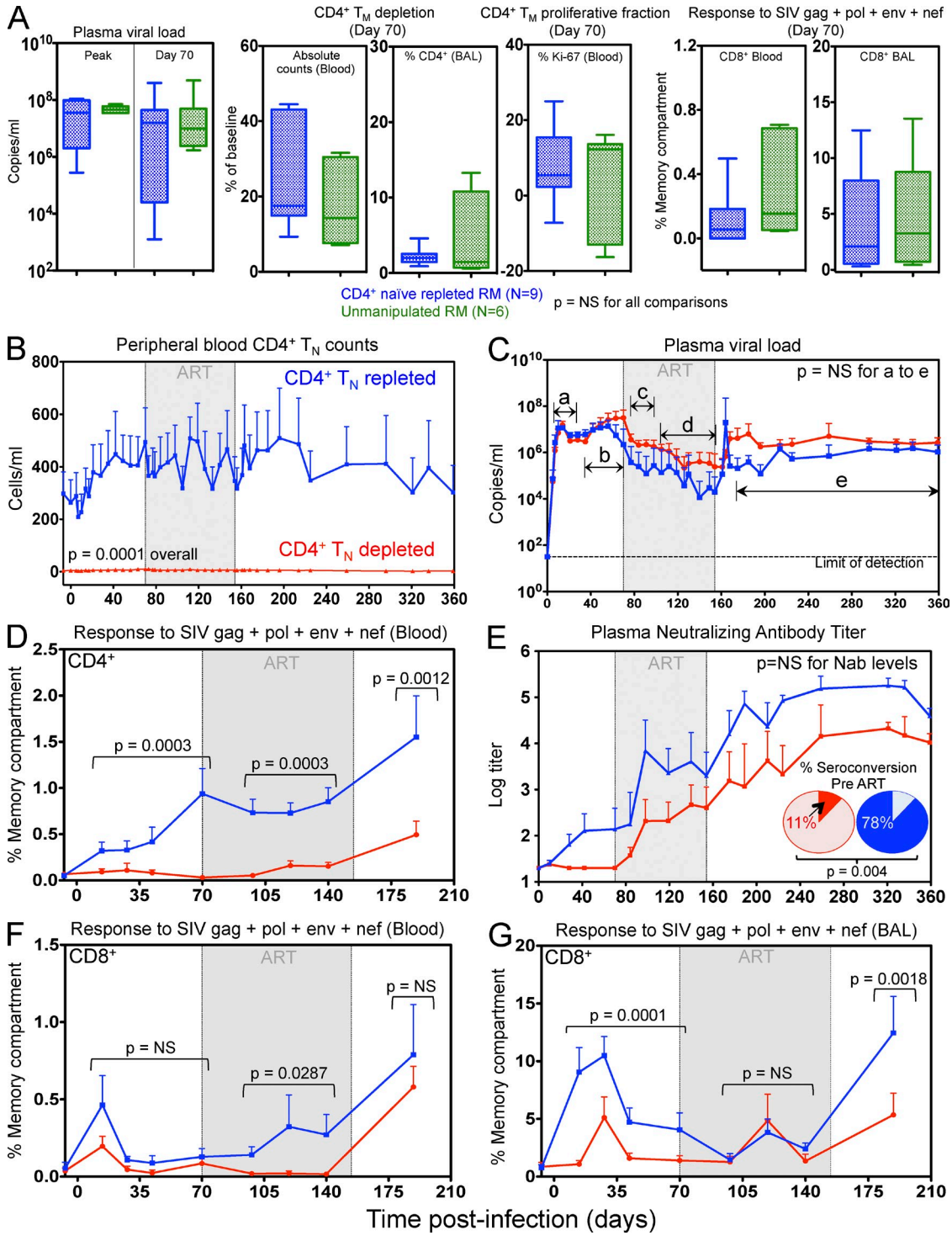

Figure 2. CD4+ T_N-deficient RMs display SIV replication dynamics similar to control RMs despite attenuated SIV-specific T cell and Ab responses. (A) Comparison of pvl, CD4+ T_M depletion, CD4+ T_M proliferative responses, and the magnitude of SIV-specific CD8+ T cell responses at day 70 pi between the CD4+ T_N -repleted control group ($n = 9$) and unmanipulated RMs ($n = 6$) challenged with the same SIVmac239 virus. Shown are box plots, with boxes and whiskers indicating interquartile ranges (25^{th}–75^{th} percentiles) and 10^{th}–90^{th} percentile values, respectively. Significance of differences in these parameters between groups was assessed as described in the Materials and methods (NS, nonsignificant). (B–G) Comparison of the indicated parameters (mean + SEM) over the course of SIVmac239 infection between the CD4+ T_N-depleted and CD4+ T_N-repleted groups ($n = 9$ each). The period over which all RMs received ART (day 70–156 pi) is shown in gray. The inset in E shows the percentage of RMs in the CD4+ T_N-depleted (red) and T_N-repleted (blue) RM groups that displayed a measureable anti-SIVenv neutralizing Ab response (e.g., seroconverted) before ART. Differences in these parameters between the CD4+ T_N-depleted and CD4+ T_N-repleted groups were statistically analyzed as described in the Materials and methods, with brackets indicating time points that were grouped together for analysis (significant p-values shown).

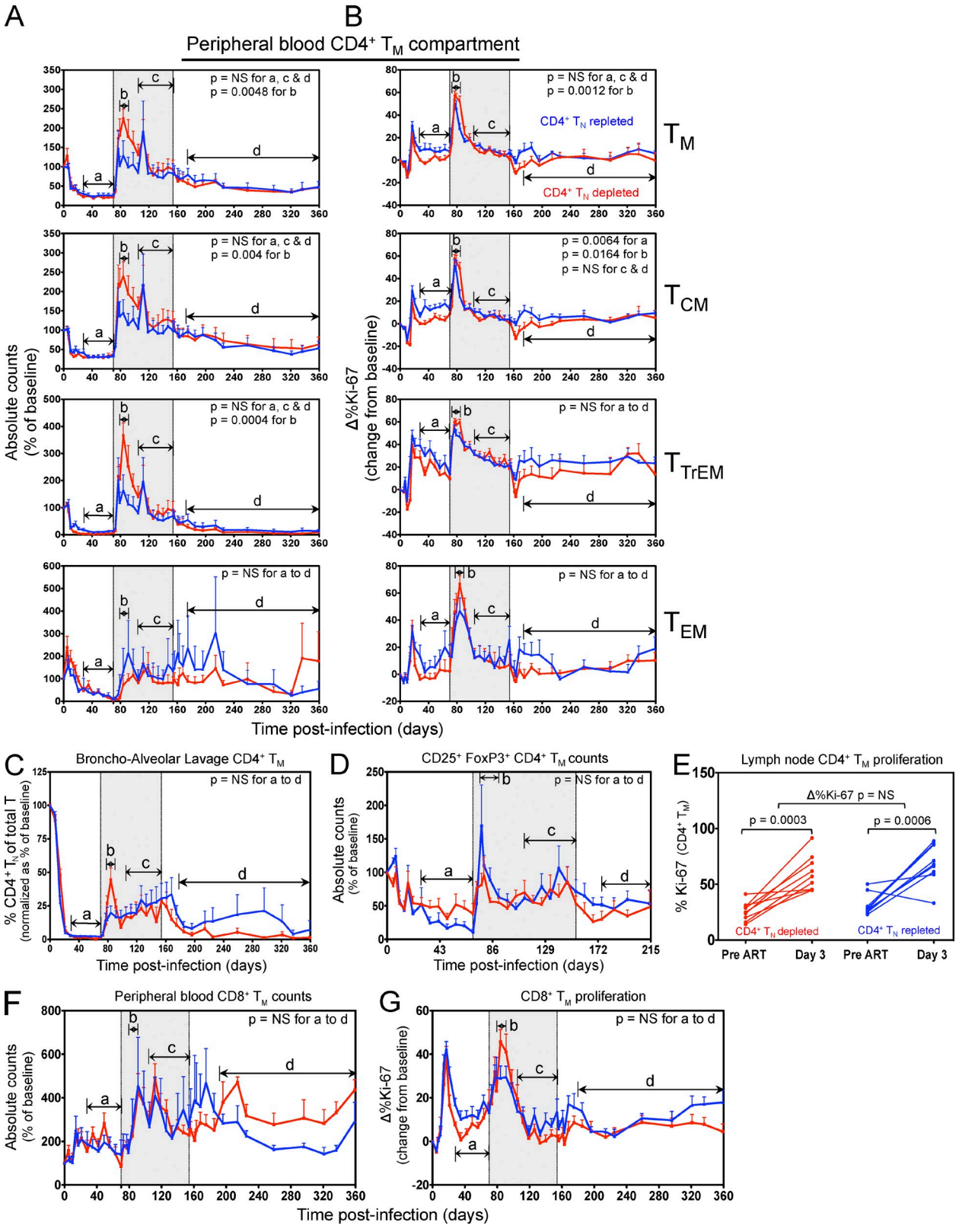

Figure 3. CD4⁺ T_N deficiency does not compromise CD4⁺ T_M homeostasis in progressive and partially suppressed SIV infection. (A–D) Comparison of the dynamics (absolute counts and proliferative fraction; mean + SEM) of overall CD4⁺ T_M and the T_{CM}, T_{TrEM}, and T_{EM} subsets in blood, the percentage of CD4⁺ of total CD3⁺ (memory) T cells in BAL, and absolute counts of CD4⁺ T_M with a regulatory phenotype (CD25⁺/FoxP3⁺) in blood of CD4⁺ T_N-depleted (red, $n = 9$) versus -repleted RMs (blue, $n = 9$) over the course of SIV infection (as in Fig. 1 A). The significance of differences in these parameters

early plateau- and chronic-phase pvl were also not significantly different between the $CD4^+$ T_N-depleted and -repleted groups (Fig. 2 C), despite the facts that SIV-specific $CD4^+$ T cell responses were essentially absent in $CD4^+$ T_N-depleted RMs during acute infection (Fig. 2 D), and that only 11% of these RMs (vs. 78% of the $CD4^+$ T_N-repleted group) showed the development of SIVenv-specific Abs by day 70 pi (Fig. 2 E, inset). The magnitude of the SIV-specific $CD8^+$ T cell response in blood also tended to be lower in the $CD4^+$ T_N-depleted RMs than in the $CD4^+$ T_N-repleted controls, but this difference achieved statistical significance only during anti-retroviral therapy (ART; Fig. 2 F). However, a significant difference in the frequency of SIV-specific $CD8^+$ T cells in $CD4^+$ T_N-depleted versus -repleted cohorts was observed in BAL during early plateau phase, as well as after ART cessation (Fig. 2 G), suggesting that SIV-specific $CD8^+$ T cell responses were compromised in the absence of $CD4^+$ T_N.

It is noteworthy that small SIV-specific $CD4^+$ T cell responses were detected over time in the $CD4^+$ T_N-depleted RMs (Fig. 2 D), suggesting that in the context of persistent Ag exposure, either residual $CD4^+$ T_N or cross-reactive $CD4^+$ T_M (Selin et al., 2006) can eventually be recruited to generate specific $CD4^+$ T cell responses in $CD4^+$ T_N-depleted RMs. ART was associated with development of SIVenv-specific Ab responses in those $CD4^+$ T_N-depleted RMs that had failed to develop these Abs before ART, although this occurred before first detection of SIV-specific $CD4^+$ T cells (Fig. 2, D and E). Titers of SIVenv-specific Abs were ~1 log higher in the $CD4^+$ T_N-repleted RMs compared with the $CD4^+$ T_N-depleted RMs throughout the course of the study, but these differences did not achieve statistical significance (Fig. 2 E).

The severe impairment of the SIV-specific $CD4^+$ T cell response in $CD4^+$ T_N-depleted versus -repleted RMs and the associated effects on the development of SIV-specific Ab and $CD8^+$ T cell responses confirms the stringency of $CD4^+$ T_N depletion in the former group (reducing SIV-specific $CD4^+$ T_N precursors below the threshold needed for a normal response) and is consistent with the previously well described importance of $CD4^+$ helper T cells to other aspects of the adaptive immune response (Behrens et al., 2004; McHeyzer-Williams et al., 2009). It is, however, remarkable that these deficits in the adaptive immune response to SIV had very little effect on SIV replication dynamics in either early plateau phase or post-ART chronic phase. This observation is consistent with the idea that absent $CD8^+$ T cell responses restricted by protective class I MHC alleles, adaptive immunity has only a limited influence on the course of highly pathogenic SIV infection of unvaccinated RMs (Picker et al., 2012). We would also note, however, that although the postpeak drop in pvl from peak to early plateau phase was relatively modest in both the $CD4^+$ T_N-depleted and -repleted groups reported here, it was still significantly greater than RMs that have been experimentally depleted of $CD8^+$ lymphocytes by anti-CD8 mAb administration during acute SIVmac239 infection, where there is typically no drop in pvl from peak levels and RMs rapidly progress to AIDS (Okoye et al., 2009). This difference, reflecting limited $CD8^+$ lymphocyte-dependent viral control, could be mediated by the relatively modest SIV-specific $CD8^+$ T cell responses observed in our RMs (including responses developing in the absence of $CD4^+$ T cell help) or, potentially, by non–Ag-specific (innate) functions of $CD8^+$ lymphocytes (T cells and/or NK cells; Okoye et al., 2009).

$CD4^+$ T_M homeostasis and disease progression in SIV-infected RMs with and without a $CD4^+$ T_N compartment

Given the statistically equivalent viral dynamics manifested by the $CD4^+$ T_N-depleted and -repleted cohorts throughout the course of infection (both on and off ART; Fig. 2 C), it is likely that the direct and indirect stress of pathogenic SIV infection on $CD4^+$ T_M homeostasis (e.g., direct viral killing or immune activation-mediated destruction and dysregulation of the $CD4^+$ T_M themselves or their supporting microenvironments; Grossman et al., 2006) was comparable for both groups. Therefore, the extent to which the $CD4^+$ T_M compartment depends on T_N recruitment in the face of this stress would be reflected by the relative ability of $CD4^+$ T_N-depleted RMs to maintain overall and proliferating $CD4^+$ T_M populations compared with the $CD4^+$ T_N-repleted RMs. Strikingly, we found no evidence of compromised homeostasis of any $CD4^+$ T_M subset in the absence of a $CD4^+$ T_N compartment, including T_{CM}, T_{TrEM}, T_{EM}, and regulatory ($CD25^+$/$FoxP3^+$) T_M populations (Fig. 3, A–D). The kinetics and extent of $CD4^+$ T_M loss in blood (all subsets) and BAL in early infection (through day 70 pi) were essentially identical between the $CD4^+$ T_N-depleted and –repleted groups (Fig. 3, A and C). Interestingly, the increase in $CD4^+$ T_M, T_{CM}, and T_{TrEM} numbers after partial inhibition of viral replication with tenofovir and emtricitabine was actually significantly higher in the $CD4^+$ T_N-depleted group, perhaps as the result of an increased availability of homeostatic cytokines such as IL-7 in the absence of a $CD4^+$ T_N population (Fig. 3 A). This difference was not maintained, however, as $CD4^+$ T_M counts equalized between the study cohorts toward the end of ART and remained equivalent during post-ART chronic infection (Fig. 3 A). The infection-associated increase in the proliferative fraction of circulating $CD4^+$ T_{CM} (but not other T_M subsets) was significantly, albeit modestly, lower in the $CD4^+$ T_N-depleted group in the early plateau phase of infection

between RM groups in the indicated regions was assessed as described in the Materials and methods (significant p-values shown; NS, nonsignificant). (E) Comparison of the change in the percentage of Ki-67^+ $CD4^+$ T_M in peripheral LN of $CD4^+$ T_N-depleted versus –repleted RMs between days 70 (ART day 0) and 73 (3 d after ART). Note that the increase in the percentage of Ki-67^+ cells from day 70 to 73 was significant in both groups (p-values shown), but the magnitude of this increase (Δ%Ki-67) was not different between groups. (F and G) Comparison of the dynamics of $CD8^+$ T_M in the blood of $CD4^+$ T_N-depleted versus –repleted RMs over the course of SIV infection (mean + SEM), with statistical analysis of the indicated regions.

(Fig. 3 B, region a), perhaps as a result of the lack of an SIV-specific $CD4^+$ T cell response in this group (which could have directly contributed to the proliferative fraction, as well as indirectly promoted nonspecific $CD4^+$ T_{CM} proliferation via elaboration of IL-2). Given the stability of T_{CM} numbers and T_{TrEM} and T_{EM} production in $CD4^+$ T_N–depleted RMs during this time period (Fig. 3, A and C), this finding does not appear to reflect impaired $CD4^+$ T_{CM} homeostasis. Moreover, the unimpaired capacity of the $CD4^+$ T_{CM} (and other $CD4^+$ T_M subsets) in $CD4^+$ T_N–depleted RMs to expand is demonstrated by the equivalently increased proliferative fraction of these cells in blood and LN after the initiation of ART (Fig. 3, B and E). Finally, $CD8^+$ T_M dynamics in blood (absolute counts and proliferative fraction) were also statistically indistinguishable between the $CD4^+$ T_N–depleted and -repleted groups (Fig. 3, F and G).

Thus, profound $CD4^+$ T_N depletion did not impair either $CD4^+$ T_{CM} homeostasis or $CD4^+$ T_{TrEM} and T_{EM} production in SIV-infected RMs, which are both parameters whose failure has been previously associated with progression to AIDS (Picker et al., 2004; Okoye et al., 2007; Grossman and Picker, 2008). To evaluate whether $CD4^+$ T_N cell deficiency was associated with accelerated disease progression, we performed statistical analysis of Kaplan-Meier plots of the time to development of end-stage (AIDS compatible) disease by log-rank test. As shown in Fig. 4 A, we found no significant difference in the time to end-stage disease between the $CD4^+$ T_N–depleted and -repleted groups. Pathological findings were consistent with end-stage simian AIDS in all RMs clinically progressing to AIDS during the study period, with no major differences in disease manifestations between groups (Fig. 4 B). At necropsy, LN of $CD4^+$ T_N–depleted RMs showed very few cells with a T_N-compatible phenotype, in contrast to $CD4^+$ T_N–repleted RMs, which showed prominent $CD4^+$ T_N populations (Fig. 4 C). To compare overall $CD4^+$ T_M depletion in these two groups that had markedly different $CD4^+$ T_N populations, we analyzed the ratio of $CD4^+$ T_M to $CD8^+$ T_M in both secondary lymphoid tissues (LN and spleen) and effector sites (BAL, liver, and small intestinal mucosa). As shown in Fig. 4 D, these ratios were not significantly different between the $CD4^+$ T_N–depleted and -repleted RMs, with both groups showing patterns typical of SIVmac239-induced AIDS (e.g., effector site $CD4^+$ T_M depletion > secondary lymphoid tissue $CD4^+$ T_M depletion; Okoye et al., 2007). Thus, the presence or absence of $CD4^+$ T_N had no measureable influence on the tempo of progression to overt immunodeficiency or the clinical/pathological manifestations of that immunodeficiency.

The lack of effect of $CD4^+$ T_N depletion on SIV control and disease progression in our study contrasts with the results of Ortiz et al. (2011), who found that all RMs infected with SIVmac251 45 d after mAb-mediated $CD4^+$ T cell depletion manifested rapid disease progression (63 d median survival) with no postpeak decline in pvl. These different outcomes almost certainly reflect fundamental differences in the approaches used to hinder $CD4^+$ T cell function in vivo. At the time of SIV infection, the $CD4^+$ T_N–depleted RMs described here were postregenerative, with baseline levels of $CD4^+$ T_M turnover. In contrast, at the start of SIV infection, the $CD4^+$ T cell–depleted RMs reported by Ortiz et al. (2011) manifested a regenerating $CD4^+$ T cell compartment with a markedly elevated proliferative fraction ($Ki\text{-}67^+$). In contrast to our findings of ablated SIV-specific $CD4^+$ T cell responses and diminished SIV-specific Ab and $CD8^+$ T cell responses in $CD4^+$ T_N–depleted RMs, Ortiz et al. (2011) reported unimpaired SIV-specific T cell ($CD4^+$ and $CD8^+$) and humoral immunity in their $CD4^+$ T cell–depleted RMs compared with controls. These observations suggest that the rapid progression observed by Ortiz et al. (2011) is most likely a consequence of the regenerative state of the $CD4^+$ T cells and/or the homeostatically activated lymphoid microenvironments in their RMs at the time of infection, rather than a direct result of deficient SIV-specific $CD4^+$ T cell immunity.

Collectively, the data presented in this report indicate that $CD4^+$ T_N are dispensable for $CD4^+$ T_M homeostasis over the relatively short course of highly pathogenic CCR5-tropic SIV infection, a conclusion which strongly argues against both a continuous replenishment of $CD4^+$ T_M by $CD4^+$ T_N recruitment and a significant role for $CD4^+$ T_N exhaustion in the pathogenesis of AIDS in SIV-infected RMs (Nishimura et al., 2007). Our analysis also suggests that initial $CD4^+$ T_M reconstitution in the setting of partially effective ART is $CD4^+$ T_N independent and, in fact, might even be transiently enhanced by the absence of $CD4^+$ T_N competition for trophic factors. These results imply that $CD4^+$ T_N may be more of a bystander to AIDS pathogenesis than previously assumed, and that dysfunction of the mechanisms responsible for intrinsic homeostasis of the $CD4^+$ T_{CM} compartment may play the dominant role in the immune degradation leading to AIDS, as well as in limitations in immune reconstitution after viral suppression. $CD4^+$ T_N depletion is clearly a prominent feature of progressive HIV infection (Khoury et al., 2011; Rickabaugh et al., 2011), and it remains possible that the lower viral replication rates and longer course of HIV infection in humans relative to SIV infection in RMs (Letvin and King, 1990) allows for $CD4^+$ T_N to make a larger contribution to immune homeostasis in HIV infection than seen in the current study. However, it must be considered that the direct $CD4^+$ T cell destruction, pathological immune activation, and microenvironmental destruction associated with HIV/SIV infection are detrimental to both $CD4^+$ T_M and T_N homeostasis (Douek et al., 2003; Grossman et al., 2006; Khoury et al., 2011; Zeng et al., 2011) and, thus, the degradation of $CD4^+$ T_N homeostasis might closely correlate with AIDS progression or immune reconstitution without being the primary mechanistic factor that determines these outcomes. The determination of the relative contribution of the $CD4^+$ T_N and T_M compartments to immune competence is of more than academic interest, as therapeutic approaches to optimally augment $CD4^+$ T_N versus T_M regeneration are likely to be different. Our data would suggest that therapies directed at correcting disturbances in $CD4^+$ T_{CM} homeostasis/regeneration might

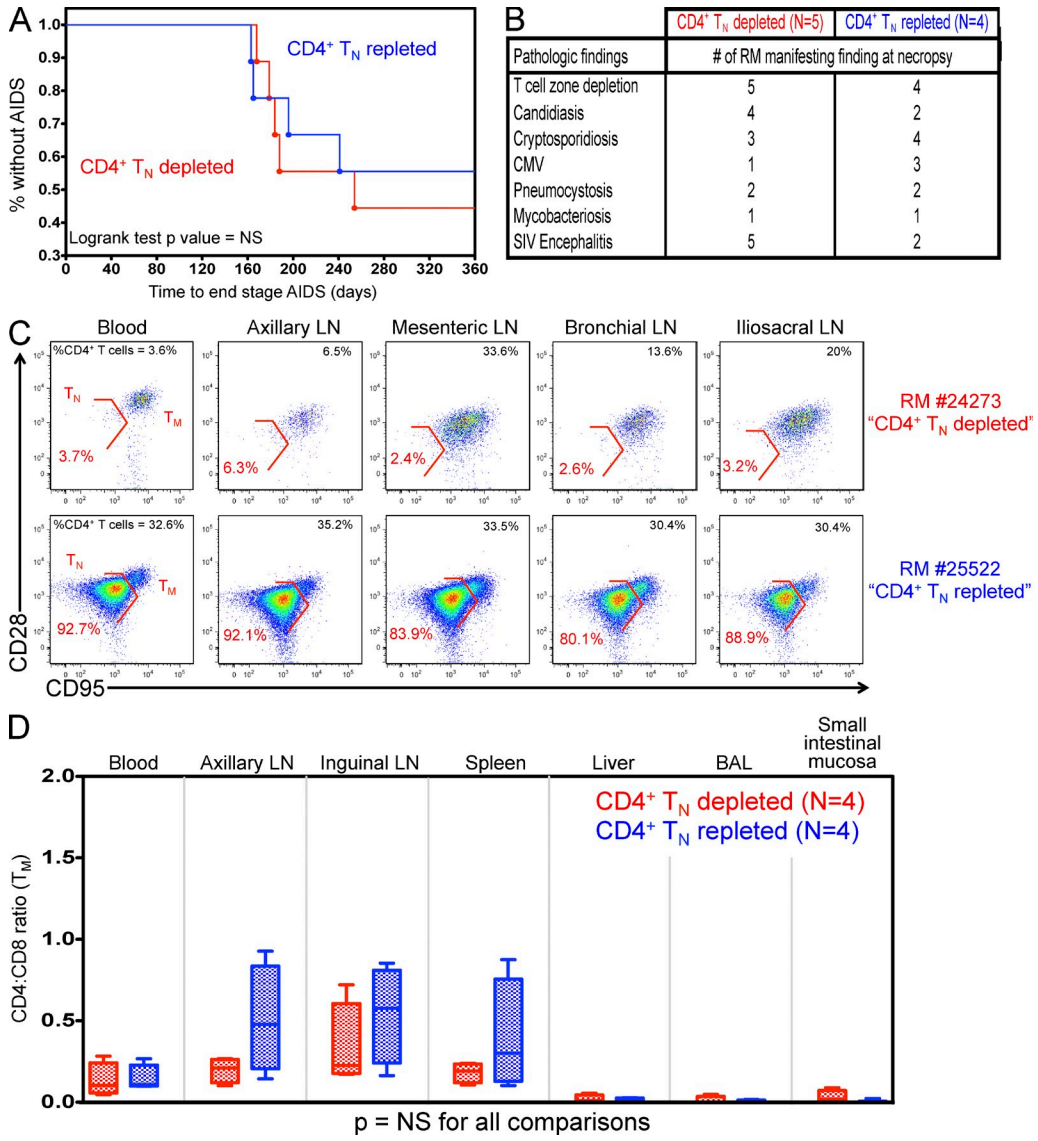

Figure 4. CD4⁺ T_N deficiency does not accelerate disease progression. (A) Kaplan-Meier plot of the time to end-stage AIDS (day of disease mandated necropsy) for CD4⁺ T_N-depleted (red, $n = 9$) versus -repleted RMs (blue, $n = 9$) over the 1 yr of follow-up. Log rank analysis indicated that rate of progression to AIDS between the two groups was not significantly different (P = 0.72). (B) Major pathological findings at necropsy of study RMs progressing to end-stage AIDS ($n = 5$ and 4 for CD4⁺ T_N-depleted vs. -repleted RMs, respectively). (C) Flow cytometric profiles (as described in Fig. 1 M) of CD4⁺ T cell populations in blood and various LNs at necropsy of representative CD4⁺ T_N-depleted (#24273, progression to AIDS at day 190 pi) and CD4⁺ T_N-repleted (#25522, progression to AIDS at day 163 pi) RMs. The percentage of T_N of gated events (total CD4⁺ T) is shown in red in the bottom left. The percentage of CD4⁺ of total T cells is shown in black at the top right. (D) Comparison of CD4⁺/CD8⁺ ratios within the T_M populations in blood and selected secondary lymphoid tissues (axillary and inguinal LNs and spleen) and effector sites (liver, BAL, and small intestinal mucosa) of four of five CD4⁺ T_N-depleted (red) and four of four CD4⁺ T_N-repleted (blue) RMs studied at necropsy (one CD4⁺ T_N-depleted RM could not be analyzed as a result of inadequate staining of cell preparations obtained at necropsy). Shown are box plots, with boxes and whiskers indicating interquartile ranges (25th–75th percentiles) and 10th–90th percentile values, respectively. Statistical analysis of differences in this parameter between groups was analyzed as described in the Materials and methods (NS, nonsignificant).

prove superior in maintaining or restoring effective immunity in HIV infection than therapies aimed at augmenting thymopoiesis or enhancing CD4⁺ T_N homeostasis.

MATERIALS AND METHODS

Animals and viruses. A total of 32 purpose-bred male juvenile RMs (*Macaca mulatta*) of Indian genetic background and free of Cercopithicine herpesvirus 1, D type simian retrovirus, simian T-lymphotrophic virus type 1, and SIV infection were used in this study. All animals were naturally infected with Rhesus CMV (RhCMV) before the start of the study. RMs with protective class 1 MHC alleles *Mamu* B*08, *Mamu* B*17, and *Mamu* A*01 were excluded from the study. A total of 26 juvenile RMs (3–5 yr old) were subjected to surgical thymectomy or sham surgery ($n = 13$ per group) before receiving the CD4⁺ T cell–depleting anti-CD4 huOKT4A mAb (Vaccari et al., 2008; Engram et al., 2010). HuOKT4A mAb was i.v. administered two times at a dose of 50 mg/kg, 1 wk apart. Four RMs from each group were excluded from the SIV infection study as a result of incomplete CD4⁺ T cell depletion in blood, leaving $n = 9$

each in the CD4+ T_N-depleted and CD4+ T_N-repleted cohorts studied after SIV infection. Postdepletion data from three thymectomized RMs with high but incomplete depletion (mean of 95% at day 21) is shown to document CD4+ T_N and T_M dynamics in RMs in which these subsets can be analyzed throughout the regeneration period. Six additional RMs were studied as unmanipulated SIV-infected controls. RMs were infected with SIVmac239 via i.v. administration of 5-ng equivalents of SIV p27, corresponding to 2.7–3.0 × 10^4 infectious centers, as previously described (Picker et al., 2004). BALs were performed as previously described (Picker et al., 2004). ART consisted of daily subcutaneous injections of 30 mg/kg 9-R-(2-phosphonomethoxypropyl) adenine (tenofovir) and 50 mg/kg β-2′,3′-dideoxy-3′-thia-5-fluorocytidine (emtricitabine). All RMs were studied at the Oregon National Primate Research Center in accordance with standards of the National Institutes of Health Guide for the Care and Use of Laboratory Animals under the approval of the Center's Animal Care and Use Committee. RMs that developed disease states that were not clinically manageable were euthanized in accordance with the recommendations of the Panel on Euthanasia of the American Veterinary Medical Association. End-stage AIDS was defined by the presence of AIDS-defining OIs, wasting syndrome unresponsive to therapy, or non-Hodgkin's lymphoma (Letvin and King, 1990).

Viral quantification. Plasma SIV RNA was assessed using a real-time RT-PCR assay (threshold sensitivity = 30 SIV gag RNA copies/ml of plasma; inter-assay CV ≤ 25%), essentially as previously described (Cline et al., 2005).

MAbs. MAbs L200 (CD4; AmCyan), SP34-2 (CD3; Alexa 700, Pacific blue), SK1 (CD8α; PerCP-Cy5.5), B56 (Ki-67; FITC), DX2 (CD95; PE, PE-Cy7), 2A3 (CD25; APC), 3A9 (CCR5; APC), and B27 (IFN-γ; APC) were obtained from BD. CD28.2 (PE-Texas red) and TP1.55.33 (CD69; PE-Texas red) were obtained from Beckman Coulter. mAb PCH101 (FoxP3; PE) and MAb111 (TNF; FITC; PE-Cy7) were obtained from eBioscience. mAb 150503 (anti-CCR7) was purchased as purified immunoglobulin from R&D Systems, conjugated to biotin using the EZ-Link Maleimide-PEO solid phase biotinylation kit (Thermo Fisher Scientific), and visualized with streptavidin–Pacific blue (Invitrogen). The depleting anti-CD4 huOKT4A mAb was provided by the National Institutes of Health Nonhuman Primate Reagent Resource Program.

Immunological assays. SIV-specific CD4+ and CD8+ T cell and RhCMV-specific CD4+ T cell responses were measured in mononuclear cell preparations from blood and tissues by flow cytometric intracellular cytokine analysis, as previously described (Hansen et al., 2009). In brief, sequential 15-mer peptides (overlapping by 11 amino acids) comprising the SIVmac239 Gag, Nef, Env, and Pol proteins or RhCMV viral lysates were used in the presence of costimulatory CD28 and CD49d monoclonal antibodies. Cells were incubated with antigen and costimulatory molecules alone for 1 h, followed by addition of Brefeldin A (Sigma-Aldrich) for an additional 8 h. Co-stimulation without antigen served as a background control. Cells were then stained with fluorochrome-conjugated monoclonal antibodies, flow cytometric data collected on an LSR II (BD), and data analyzed using the FlowJo software program (version 8.8.6; Tree Star). Response frequencies (CD69+/TNF+ and/or CD69+/IFN-γ+) were first determined in the overall CD4+ and CD8+ population and then memory corrected (with memory T cell subset populations delineated on the basis of CD28 and CD95 expression), as previously described (Hansen et al., 2010). Neutralizing Abs against tissue culture-adapted SIVmac251 were measured in luciferase reporter gene assays using the TZM-bl cells for tissue culture–adapted SIVmac251 (Montefiori, 2005).

Flow cytometric analysis. Whole blood, PBMC, LN, BAL, and small intestinal mucosa cells were obtained and stained for flow cytometric analysis as previously described (Pitcher et al., 2002; Picker et al., 2004). Polychromatic (8–12 parameter) flow cytometric analysis was performed on an LSR II instrument using Pacific blue, AmCyan, FITC, PE, PE–Texas red, PE-Cy7, PerCP-Cy5.5, APC, APC-Cy7, and Alexa Fluor 700 as the available fluorescent parameters. To evaluate FoxP3 expression, whole blood was obtained and stained with anti-CD3-A700, CD4-AmCyan, CD8-PerCP-Cy5.5, CD28.2-PE–Texas red, CD95-PE-Cy7, CCR7-Biotin–Pacific blue, and CD25-APC antibodies, fixed and permeabilized using the FoxP3 whole blood staining kit (eBioscience), and then stained with FoxP3-PE and Ki-67-FITC. Instrument set-up and data acquisition procedures were performed as previously described (Walker et al., 2004). List mode multiparameter data files were analyzed using FlowJo software. Criteria for delineating naive and memory T cell subsets and for setting + versus − markers for CCR5 and Ki-67 expression have been previously described in detail (Pitcher et al., 2002; Picker et al., 2004; Grossman and Picker, 2008). In brief, T_N constitute a uniform cluster of cells with a $CD28^{moderate}$, CCR7+, CCR5−, $CD95^{low}$ phenotype, which is clearly distinguishable from the phenotypically diverse memory population that is $CD95^{high}$ or displays one or more of the following non-naive phenotypic features: CD28−, CCR7−, or CCR5+. The T_{CM}, T_{TrEM}, and T_{EM} cell components of the memory subset in the blood and LNs were further delineated based on the following phenotypic criteria: T_{CM} (CD28+, and CCR7+ and CCR5−), T_{TrEM} (CD28+, and CCR7− and/or CCR5+), and T_{EM} (CD28−, and CCR7− and $CCR5^{dim}$). For each subset to be quantified, the percentages of the subset within the overall small lymphocyte and/or small T cell (CD3+ small lymphocyte) populations were determined. For quantification of peripheral blood subsets, absolute small lymphocyte counts were obtained using an AcT5diff cell counter (Beckman Coulter) and, from these values, absolute counts for the relevant subset were calculated based the subset percentages within the light scatter–defined small lymphocyte population on the flow cytometer. Results (absolute subset counts after CD4+ cell depletion or after SIV infection) are presented as percentage of baseline, with baseline determined as the mean of values determined at days −14, −7, and 0 relative to the first dose of huOKT4A or to SIV challenge. For quantification in tissue, the fraction of the relevant subset within the overall T cell compartment after depletion or after SIV challenge was directly normalized to the baseline fraction, and the results were presented as percentage of baseline. For LN and intestinal biopsies, only one baseline sample was available.

Statistical analysis. Repeated measures ANOVA was used to investigate the effect of thymectomy versus sham surgery on T cell reconstitution after mAb huOKT4-mediated CD4+ T cell depletion, and the effects of CD4+ T_N deficiency on pvl and T cell subset/response dynamics after SIV infection. First order autoregressive covariance structure was used to account for within-subject correlation. Bonferroni's multiple comparison adjustment for preplanned contrasts was applied to secure overall type I error, whereas false discovery rate method for multiple comparison adjustment was applied for pairwise comparisons to avoid over-adjustment. Wilcoxon rank sum tests were used to compare the difference between CD4+ naive-repleted RMs and unmanipulated RMs in pvl (peak and day 70 pi), CD4+ T_M depletion (blood and BAL), CD4+ T_M proliferative response (blood), and the magnitude of SIV-specific CD8+ T cell responses at day 70 pi (blood and BAL) and to compare pre-challenge frequencies of RhCMV-specific CD4+ T cells between the CD4+ naive-depleted and -repleted RMs. The log-rank test was used to compare the survival distributions between CD4+ T_N–depleted and -repleted RMs along the Kaplan-Meier curve. Logistic regression was used to access a difference in the fraction of RMs in each group manifesting measureable SIVenv-specific Ab titers by day 70 pi (binary outcome: responder vs. nonresponder). Permutation test was used to compare the statistical significance difference of CD4+/CD8+ ratios within the T cell memory populations in blood and selected secondary lymphoid tissues (axillary and inguinal LNs and spleen) and effector sites (liver, BAL, and small intestinal mucosa) of four out of five CD4+ T_N–depleted and four out of four CD4+ T_N–repleted RMs. Statistical significance was determined at the significance level of 0.05. These analyses were conducted using the Statistical Analysis System version 9.2 software.

The authors thank N. Whizin, J. Clock, D. Duell, D. Siess, S. Hagen, Q. DeGottardi, S. Hansen, and H. Park for specialized technical assistance, K. Reimann and The Nonhuman Primate Reagent Resource Program for the humanized monoclonal anti-CD4 antibody huOKT4A, D. Watkins for MHC typing, and D. Montefiori for neutralizing Ab assays.

This work was supported by National Institutes of Health grants R37-AI054292 and P51-RR00163 and federal funds from the National Cancer Institute, National Institutes of Health, under Contract No. HHSN261200800001E.

The authors declare no competing financial interests.

Submitted: 28 September 2011
Accepted: 21 February 2012

REFERENCES

Arron, S.T., R.M. Ribeiro, A. Gettie, R. Bohm, J. Blanchard, J. Yu, A.S. Perelson, D.D. Ho, and L. Zhang. 2005. Impact of thymectomy on the peripheral T cell pool in rhesus macaques before and after infection with simian immunodeficiency virus. *Eur. J. Immunol.* 35:46–55. http://dx.doi.org/10.1002/eji.200424996

Behrens, G., M. Li, C.M. Smith, G.T. Belz, J. Mintern, F.R. Carbone, and W.R. Heath. 2004. Helper T cells, dendritic cells and CTL Immunity. *Immunol. Cell Biol.* 82:84–90. http://dx.doi.org/10.1111/j.1440-1711.2004.01211.x

Brenchley, J.M., T.W. Schacker, L.E. Ruff, D.A. Price, J.H. Taylor, G.J. Beilman, P.L. Nguyen, A. Khoruts, M. Larson, A.T. Haase, and D.C. Douek. 2004. $CD4^+$ T cell depletion during all stages of HIV disease occurs predominantly in the gastrointestinal tract. *J. Exp. Med.* 200:749–759. http://dx.doi.org/10.1084/jem.20040874

Catalfamo, M., C. Wilhelm, L. Tcheung, M. Proschan, T. Friesen, J.H. Park, J. Adelsberger, M. Baseler, F. Maldarelli, R. Davey, et al. 2011. CD4 and CD8 T cell immune activation during chronic HIV infection: roles of homeostasis, HIV, type I IFN, and IL-7. *J. Immunol.* 186:2106–2116. http://dx.doi.org/10.4049/jimmunol.1002000

Cline, A.N., J.W. Bess, M. Piatak Jr., and J.D. Lifson. 2005. Highly sensitive SIV plasma viral load assay: practical considerations, realistic performance expectations, and application to reverse engineering of vaccines for AIDS. *J. Med. Primatol.* 34:303–312. http://dx.doi.org/10.1111/j.1600-0684.2005.00128.x

Douek, D.C., L.J. Picker, and R.A. Koup. 2003. T cell dynamics in HIV-1 infection. *Annu. Rev. Immunol.* 21:265–304. http://dx.doi.org/10.1146/annurev.immunol.21.120601.141053

Engram, J.C., B. Cervasi, J.A. Borghans, N.R. Klatt, S.N. Gordon, A. Chahroudi, J.G. Else, R.S. Mittler, D.L. Sodora, R.J. de Boer, et al. 2010. Lineage-specific T-cell reconstitution following in vivo $CD4^+$ and $CD8^+$ lymphocyte depletion in nonhuman primates. *Blood.* 116:748–758. http://dx.doi.org/10.1182/blood-2010-01-263814

Gattinoni, L., E. Lugli, Y. Ji, Z. Pos, C.M. Paulos, M.F. Quigley, J.R. Almeida, E. Gostick, Z. Yu, C. Carpenito, et al. 2011. A human memory T cell subset with stem cell-like properties. *Nat. Med.* 17:1290–1297. http://dx.doi.org/10.1038/nm.2446

Grossman, Z., and L.J. Picker. 2008. Pathogenic mechanisms in simian immunodeficiency virus infection. *Curr. Opin. HIV AIDS.* 3:380–386. http://dx.doi.org/10.1097/COH.0b013e3282fbaae6

Grossman, Z., M. Meier-Schellersheim, W.E. Paul, and L.J. Picker. 2006. Pathogenesis of HIV infection: what the virus spares is as important as what it destroys. *Nat. Med.* 12:289–295. http://dx.doi.org/10.1038/nm1380

Hansen, S.G., C. Vieville, N. Whizin, L. Coyne-Johnson, D.C. Siess, D.D. Drummond, A.W. Legasse, M.K. Axthelm, K. Oswald, C.M. Trubey, et al. 2009. Effector memory T cell responses are associated with protection of rhesus monkeys from mucosal simian immunodeficiency virus challenge. *Nat. Med.* 15:293–299. http://dx.doi.org/10.1038/nm.1935

Hansen, S.G., C.J. Powers, R. Richards, A.B. Ventura, J.C. Ford, D. Siess, M.K. Axthelm, J.A. Nelson, M.A. Jarvis, L.J. Picker, and K. Früh. 2010. Evasion of $CD8^+$ T cells is critical for superinfection by cytomegalovirus. *Science.* 328:102–106. http://dx.doi.org/10.1126/science.1185350

Khoury, G., R. Rajasuriar, P.U. Cameron, and S.R. Lewin. 2011. The role of naïve T-cells in HIV-1 pathogenesis: an emerging key player. *Clin. Immunol.* 141:253–267. http://dx.doi.org/10.1016/j.clim.2011.09.002

Letvin, N.L., and N.W. King. 1990. Immunologic and pathologic manifestations of the infection of rhesus monkeys with simian immunodeficiency virus of macaques. *J. Acquir. Immune Defic. Syndr.* 3:1023–1040.

Mason, R.D., R.D. Rose, N. Seddiki, A.D. Kelleher, and S.J. Kent. 2008. Low pre-infection levels and loss of central memory $CD4^+$ T cells may predict rapid progression in SIV-infected pigtail macaques. *Virology.* 381:11–15. http://dx.doi.org/10.1016/j.virol.2008.08.042

Mattapallil, J.J., D.C. Douek, B. Hill, Y. Nishimura, M. Martin, and M. Roederer. 2005. Massive infection and loss of memory $CD4^+$ T cells in multiple tissues during acute SIV infection. *Nature.* 434:1093–1097. http://dx.doi.org/10.1038/nature03501

McHeyzer-Williams, L.J., N. Pelletier, L. Mark, N. Fazilleau, and M.G. McHeyzer-Williams. 2009. Follicular helper T cells as cognate regulators of B cell immunity. *Curr. Opin. Immunol.* 21:266–273. http://dx.doi.org/10.1016/j.coi.2009.05.010

Montefiori, D.C. 2005. Evaluating neutralizing antibodies against HIV, SIV, and SHIV in luciferase reporter gene assays. *Curr. Protoc. Immunol.* Chapter 12:12: 11.

Nishimura, Y., T. Igarashi, A. Buckler-White, C. Buckler, H. Imamichi, R.M. Goeken, W.R. Lee, B.A. Lafont, R. Byrum, H.C. Lane, et al. 2007. Loss of naïve cells accompanies memory $CD4^+$ T-cell depletion during long-term progression to AIDS in Simian immunodeficiency virus-infected macaques. *J. Virol.* 81:893–902. http://dx.doi.org/10.1128/JVI.01635-06

Okoye, A., M. Meier-Schellersheim, J.M. Brenchley, S.I. Hagen, J.M. Walker, M. Rohankhedkar, R. Lum, J.B. Edgar, S.L. Planer, A. Legasse, et al. 2007. Progressive $CD4^+$ central memory T cell decline results in $CD4^+$ effector memory insufficiency and overt disease in chronic SIV infection. *J. Exp. Med.* 204:2171–2185. http://dx.doi.org/10.1084/jem.20070567

Okoye, A., H. Park, M. Rohankhedkar, L. Coyne-Johnson, R. Lum, J.M. Walker, S.L. Planer, A.W. Legasse, A.W. Sylwester, M. Piatak Jr., et al. 2009. Profound $CD4^+/CCR5^+$ T cell expansion is induced by $CD8^+$ lymphocyte depletion but does not account for accelerated SIV pathogenesis. *J. Exp. Med.* 206:1575–1588. http://dx.doi.org/10.1084/jem.20090356

Ortiz, A.M., N.R. Klatt, B. Li, Y. Yi, B. Tabb, X.P. Hao, L. Sternberg, B. Lawson, P.M. Carnathan, E.M. Cramer, et al. 2011. Depletion of $CD4^+$ T cells abrogates post-peak decline of viremia in SIV-infected rhesus macaques. *J. Clin. Invest.* 121:4433–4445. http://dx.doi.org/10.1172/JCI46023

Picker, L.J., S.I. Hagen, R. Lum, E.F. Reed-Inderbitzin, L.M. Daly, A.W. Sylwester, J.M. Walker, D.C. Siess, M. Piatak Jr., C. Wang, et al. 2004. Insufficient production and tissue delivery of $CD4^+$ memory T cells in rapidly progressive simian immunodeficiency virus infection. *J. Exp. Med.* 200:1299–1314. http://dx.doi.org/10.1084/jem.20041049

Picker, L.J., S.G. Hansen, and J.D. Lifson. 2012. New paradigms for HIV/AIDS vaccine development. *Annu. Rev. Med.* 63:95–111. http://dx.doi.org/10.1146/annurev-med-042010-085643

Pitcher, C.J., S.I. Hagen, J.M. Walker, R. Lum, B.L. Mitchell, V.C. Maino, M.K. Axthelm, and L.J. Picker. 2002. Development and homeostasis of T cell memory in rhesus macaque. *J. Immunol.* 168:29–43.

Rickabaugh, T.M., R.D. Kilpatrick, L.E. Hultin, P.M. Hultin, M.A. Hausner, C.A. Sugar, K.N. Althoff, J.B. Margolick, C.R. Rinaldo, R. Detels, et al. 2011. The dual impact of HIV-1 infection and aging on naïve CD4 T-cells: additive and distinct patterns of impairment. *PLoS ONE.* 6:e16459. http://dx.doi.org/10.1371/journal.pone.0016459

Selin, L.K., M.A. Brehm, Y.N. Naumov, M. Cornberg, S.K. Kim, S.C. Clute, and R.M. Welsh. 2006. Memory of mice and men: $CD8^+$ T-cell cross-reactivity and heterologous immunity. *Immunol. Rev.* 211:164–181. http://dx.doi.org/10.1111/j.0105-2896.2006.00394.x

Sener, A., A.L. Tang, and D.L. Farber. 2009. Memory T-cell predominance following T-cell depletional therapy derives from homeostatic expansion of naive T cells. *Am. J. Transplant.* 9:2615–2623. http://dx.doi.org/10.1111/j.1600-6143.2009.02820.x

Vaccari, M., J. Mattapallil, K. Song, W.P. Tsai, A. Hryniewicz, D. Venzon, M. Zanetti, K.A. Reimann, M. Roederer, and G. Franchini. 2008. Reduced protection from simian immunodeficiency virus SIVmac251 infection afforded by memory $CD8^+$ T cells induced by vaccination during $CD4^+$ T-cell deficiency. *J. Virol.* 82:9629–9638. http://dx.doi.org/10.1128/JVI.00893-08

Vezys, V., D. Masopust, C.C. Kemball, D.L. Barber, L.A. O'Mara, C.P. Larsen, T.C. Pearson, R. Ahmed, and A.E. Lukacher. 2006. Continuous recruitment of naive T cells contributes to heterogeneity of antiviral CD8 T cells during persistent infection. *J. Exp. Med.* 203:2263–2269. http://dx.doi.org/10.1084/jem.20060995

Walker, J.M., H.T. Maecker, V.C. Maino, and L.J. Picker. 2004. Multicolor flow cytometric analysis in SIV-infected rhesus macaque. *Methods Cell Biol.* 75:535–557. http://dx.doi.org/10.1016/S0091-679X(04)75022-0

Zeng, M., A.J. Smith, S.W. Wietgrefe, P.J. Southern, T.W. Schacker, C.S. Reilly, J.D. Estes, G.F. Burton, G. Silvestri, J.D. Lifson, et al. 2011. Cumulative mechanisms of lymphoid tissue fibrosis and T cell depletion in HIV-1 and SIV infections. *J. Clin. Invest.* 121:998–1008. http://dx.doi.org/10.1172/JCI45157